Convergent evolution of plant pattern recognition receptors sensing cysteine-rich patterns from three microbial kingdoms

Yuankun Yang[1,9]*, Christina E. Steidele[1,2,9], Birgit Löffelhardt[1], Dagmar Kolb[1], Thomas Leisen[3], Weiguo Zhang[1,4], Christina Ludwig[5], Georg Felix[1], Michael F. Seidl[6,7], Thorsten Nürnberger[1], Matthias Hahn[3], Bertolt Gust[8], Harald Gross[8], Ralph Hückelhoven[2], Andrea A. Gust[1]*

[1]Department of Plant Biochemistry, Centre of Plant Molecular Biology (ZMBP), Eberhard-Karls-University of Tübingen, Tübingen, Germany.

[2]Chair of Phytopathology, School of Life Sciences Weihenstephan, Technische Universität München, Freising-Weihenstephan, Germany.

[3]Department of Biology, Phytopathology group, Technical University of Kaiserslautern, Kaiserslautern, Germany.

[4]Faculty of Life Science, Northwest University, Xi'an, China.

[5]Bavarian Center for Biomolecular Mass Spectrometry, School of Life Sciences Weihenstephan, Technische Universität München, Freising-Weihenstephan, Germany.

[6]Theoretical Biology & Bioinformatics, Department of Biology, Utrecht University, Utrecht, The Netherlands.

[7]Laboratory of Phytopathology, Wageningen University & Research, Wageningen, The Netherlands.

[8]Department of Pharmaceutical Biology, Pharmaceutical Institute, Eberhard-Karls-University of Tübingen, Tübingen, Germany.

[9]These authors contributed equally: Yuankun Yang, Christina Steidele

*For correspondence: andrea.gust@zmbp.uni-tuebingen.de; yuankun.yang@zmbp.uni-tuebingen.de

ORCID: G. Felix (0000-0002-6746-6185), A.A. Gust (0000-0003-0466-2792), B. Gust (0000-0002-1265-0065), H. Gross (0000-0002-0731-821X), M. Hahn (0000-0002-5213-9034), R. Hückelhoven (0000-0001-5632-5451), T. Leisen (0000-0003-0552-0323), C. Ludwig (0000-0002-6131-7322), T. Nürnberger (0000-0002-7804-7170), M.F. Seidl (0000-0002-5218-2083), C.E. Steidele (0000-0003-1284-6604), Y. Yang (0000-0003-3566-351X), W. Zhang (0000-0002-6504-5475)

Abstract

The *Arabidopsis thaliana* receptor-like protein RLP30 contributes to immunity against the fungal pathogen *Sclerotinia sclerotiorum*. Here we identified the RLP30-ligand as a small cysteine-rich protein (SCP) that occurs in many fungi and oomycetes and is also recognized by the *Nicotiana benthamiana* RLP RE02. However, RLP30 and RE02 share little sequence similarity and respond to different parts of the native/folded protein. Interestingly, some Brassicaceae other than Arabidopsis also respond to a linear SCP peptide, suggesting that SCP is an eminent immune target that led to the convergent evolution of distinct immune receptors in plants. Surprisingly, RLP30 shows a second ligand specificity for a SCP-nonhomologous protein secreted by bacterial Pseudomonads. RLP30 expression in *N. tabacum* resulted in lower susceptibility to bacterial, fungal and oomycete pathogens, thus demonstrating that detection of immunogenic patterns by Arabidopsis RLP30 is involved in defense against pathogens from three microbial kingdoms.

Introduction

To survive attacks by harmful microbes, plants have evolved a multifaceted innate immune system[1-3]. Pattern recognition receptors (PRRs) that perceive pathogen/microbe-associated molecular patterns (PAMPs/MAMPs) at the plasma membrane play an important role in this system to initiate active defense responses[3-6]. Many PRRs contain leucine-rich repeat (LRR) ectodomains. Based on the presence or absence of a cytoplasmic kinase domain, these LRR-PRRs can be classified as receptor kinases (LRR-RKs) or receptor-like proteins (LRR-RPs), respectively[3-6]. Immunity-related LRR-RPs form constitutive complexes with the common adaptor kinase SOBIR1 (SUPPRESSOR OF BRASSINOSTEROID INSENSITIVE 1 (BRI1)-ASSOCIATED KINASE (BAK1)-INTERACTING RECEPTOR KINASE 1), thus forming bi-molecular equivalents of LRR-RKs[4,7]. Upon binding their specific PAMP ligands, the LRR-RP/SOBIR1 complexes, much like the LRR-RKs, recruit co-receptors of the SERK (SOMATIC EMBRYOGENESIS RECEPTOR KINASE) family such as BAK1 for activation of intracellular immune signaling and induction of defense responses[4,8].

2

Over the past decades, a number of PAMPs/PRRs pairs have been identified[3,4,6,9] and most of these PAMPs occur only in a single kingdom of microorganisms. However, there are notable exceptions including the XEG1-type glucanohydrolases and the VmE02-type cysteine-rich proteins which are conserved in many plant-pathogenic fungi and oomycetes, or NLPs (NEP1-(NECROSIS AND ETHYLENE-INDUCING PEPTIDE 1)-LIKE PROTEINS) which are present in bacterial, fungal and oomycete species[10-13].

Perception of most PAMPs is restricted to closely related species, reflecting a vast diversity in the repertoires of PRRs between plant families. Restriction to closely related species holds for LRR-RP-type PRRs of Arabidopsis, including RLP23, RLP32 and RLP42, which sense nlp20, proteobacterial TRANSLATION INITIATION FACTOR 1 (IF1) and fungal polygalacturonases (PGs), respectively[4,14,15]. These LRR-RPs have no obvious homologs in species outside the Brassicaceae family. Likewise, LRR-RPs identified in solanaceous plants such as tomato, including EIX2 (ETHLYENE-INDUCING XYLANASE RECEPTOR 2) and the Cf proteins detecting effectors from *Cladosporium fulvum* have no counterparts in species of other plant families[4]. Intriguingly, detection of only a few PAMPs, notably bacterial flagellin by FLAGELLIN-SENSING 2 (FLS2) and fungal chitin by CHITIN-ELICITOR RECEPTOR KINASE 1 (CERK1), occurs in a broad range of plant species[16,17].

The *Arabidopsis* Receptor-Like Protein 30 (RLP30) mediates basal resistance to the fungus *Sclerotinia sclerotiorum* but the identity of the proteinaceous PAMP detected by RLP30 remained open[18]. Here, we report the identification of this factor as a SMALL CYSTEINE-RICH PROTEIN (SCP) closely related to VmE02 from *Valsa mali*[12]. Apart from sensing SCPs from different fungi and oomycetes, RLP30 can recognize an SCP-unrelated pattern from *Pseudomonas* bacteria and confers increased resistance to *Nicotiana tabacum* plants. We further reveal distinct immune-sensing mechanisms for SCPs in Brassicaceae and Solanaceae species. Our findings unveil an unanticipated complex relationship between PRRs and PAMPs where a single PRR recognizes PAMPs from microorganisms of three kingdoms and where a single PAMP is detected by PRRs from different plant species.

Results and Discussion

SCP^{Ss} is the immunogenic pattern secreted by *S. sclerotiorum*

The *Arabidopsis* RLP30 detects a proteinaceous elicitor secreted by *S. sclerotiorum*[18]. To identify this PAMP, originally termed SCFE1, we re-purified the activity from the supernatants of fungal cultures by an extended purification protocol and monitored its RLP30-dependent induction of the plant stress hormone ethylene (Extended Data Fig. 1a,b). Mass spectrometric analysis of the trypsin fragments obtained with the purified fractions revealed the presence of a small cysteine-rich protein (Sscle06g048920; SMALL CYSTEINE-RICH PROTEIN FROM *S. SCLEROTIORUM*, SCP^{Ss}) of 147 amino acids containing eight cysteine residues but no known protein domains (Supplementary Table 1 and Extended Data Fig. 1c). To confirm SCP^{Ss} as the ligand of RLP30, the SCP^{Ss} protein was heterologously expressed in *N. benthamiana* or *Pichia pastoris* (Extended Data Fig. 1d,e), with C-terminal GFP or His tags, respectively. Both forms were found to induce ethylene production in *Arabidopsis* Col-0 wild-type plants but not in the *rlp30-2* mutant (Fig. 1a and Extended Data Fig. 1f). His-tagged SCP^{Ss}, affinity purified via His-Trap columns, triggered ethylene production in Col-0 plants at nanomolar concentrations with a half-maximal induction (EC$_{50}$) at ~26 nM (Extended Data Fig. 2a). In contrast to *rlp30-2* mutants, Col-0 wild-type plants and *rlp30-2* mutants complemented with RLP30 responded to the SCP^{Ss} preparations with typical PAMP responses such as induction of reactive oxygen species (ROS), activation of mitogen-activated protein kinases (MAPK), and a generally induced state of resistance, supported by significantly reduced colonization by the fungus *Botrytis cinerea* or the bacterial pathogen *Pseudomonas syringae* pv. *tomato* (*Pst*) DC3000 (Fig. 1b,c and Extended Data Fig. 2b,c). Unlike most other known patterns recognized by RLPs, SCP^{Ss} did not only elicit ethylene production in *Arabidopsis* and related *Brassica species*, but also in solanaceous plants such as *N. benthamiana*, tomato, pepper, and potato (Fig. 1d).

To assess whether SCP^{Ss} interacts with RLP30, co-immunoprecipitation assays were performed with extracts from *N. benthamiana* leaves that were transiently co-transformed with myc-tagged SCP^{Ss} and with either GFP-tagged RLP30 or the GFP-tagged nlp20 receptor RLP23[19] as control. SCP^{Ss}-myc co-precipitated specifically with RLP30 but not with the structurally related RLP23 (Fig. 1e).

Several Arabidopsis accessions that were found to exhibit no response to *S. sclerotiorum* extracts carry SNPs in their *RLP30* genes leading to single amino acid changes[18]. In an extended screen with 77 accessions, we identified further accessions that did not respond to SCP*Ss* and that carried point mutations in *RLP30* (Extended Data Fig. 3a). We tested the altered RLP30 versions occurring in accessions Mt-0, Br-0, Lov-1, Lov-5, ICE111 and Sq-1 in a co-precipitation assay for binding of SCP*Ss*. While all receptor versions were expressed in *N. benthamiana*, none of them precipitated SCP*Ss* (Extended Data Fig. 3b). Thus, the single amino acid substitutions in different parts of the LRR domain (Extended Data Fig. 4a), which are specific to SCP*Ss*-responsive RLP30 variants[18], such as L307R in Mt-0, G563V in Br-0, R433G in Lov-1, Lov-5 and ICE111, and S654Y in Sq-1, respectively, all affect ligand binding and, likely, are responsible for the non-functionality of these mutated receptors.

RLP30 detects SCPs from fungi and oomycetes

Homologs of SCP*Ss* exist in many fungi and oomycetes[12]. They typically contain a predicted signal peptide, seven conserved motifs (R1 to R7) and eight conserved cysteine residues (Extended Data Fig. 5a), however, the absence of previously characterized protein domains hampers the prediction of their specific biological functions. While some SCPs have been reported to function as virulence factors with multiple strategies[20], deletion of the *SCP*Ss*-homolog in *B. cinerea* (*SCP*Bc*/Bcplp1*) or its homolog *VmE02* in *V. mali* did not alter pathogenicity on various plants[12,21] (Extended Data Fig. 5b,c), suggesting that these proteins either do not contribute significantly to virulence or act redundantly with others during infection. To assess whether SCP*Ss* homologs from other fungi and oomycetes display RLP30-dependent PAMP activity, homologs from *B. cinerea* (SCP*Bc*) and *Phytophthora infestans* (SCP*Pi*) were produced in *P. pastoris* (Extended Data Fig. 1e). Similar to SCP*Ss*, SCP*Bc* and SCP*Pi* induced the production of ethylene and MAPK activation in wild-type or *rlp30-2*/RLP30-YFP plants, but not in *rlp30-2, sobir1-12* or *bak1–5 bkk1–1* mutants or in SCP*Ss*-insensitive accessions (Fig. 2a and Extended Data Fig. 5d,e). Together, these data demonstrate that SCP*Ss* homologs, common among fungi and oomycetes, are perceived by the RLP30/SOBIR1/BAK1 receptor complex in Arabidopsis.

5

SCP^{Ss} is sensed by RE02 in *N. benthamiana*

SCP^{Ss} recognition systems are present in both Brassicaceae and Solanaceae (Fig. 1e), yet, reciprocal sequence similarity searches suggest absence of RLP30 from Solanaceae. The *N. benthamiana* receptor-like protein RE02 (Response to VmE02, 24.18 % identity to RLP30, Extended Data Fig. 4a,b) was recently identified to mediate the perception of VmE02, a cysteine-rich PAMP derived from *V. mali* with 55% identity to SCP^{Ss} [12,22]. To compare the ligand specificity of RE02 with RLP30, *RE02* expression in *N. benthamiana* was targeted by virus-induced gene silencing (VIGS), resulting in almost complete loss of SCP^{Ss}-induced ethylene production (Fig. 2b and Extended Data Fig. 6a). In contrast, leaves of silenced plants, either transiently transformed with *RE02*-GFP or *RLP30*-GFP exhibited clear SCP^{Ss} sensitivity (Fig. 2b and Extended Data Fig. 6b). Likewise, stable expression of *RE02*–GFP also reconstituted responsiveness to SCP^{Ss} in *Arabidopsis rlp30-2* mutants (Fig. 2c and Extended Data Fig. 6c). Hence, SCP^{Ss} recognition is mediated by RE02 in *N. benthamiana.*

Distinct perception of SCPs in Brassicaceae and Solanaceae

Immunogenic activity of SCP^{Ss} is sensitive to treatment with DTT (Extended Data Fig. 7a), suggesting that perception by the RLPs RLP30 and RE02 depends on the tertiary structure of SCP^{Ss}. The SCP^{Ss} protein is predicted to form four disulfide bonds (DB), most likely connecting cysteine residues C1 and C4, C2 and C3, C5 and C8 and C6 and C7, respectively (Fig. 3a). Replacing individual cysteine residues with serine leads to loss of activity on RLP30 for all eight substitutions (Fig. 3b and Extended Data Fig. 7b). When testing the individual Cys substitutions for ethylene-inducing activity in *N. benthamiana* or tomato, we observed that only the four N-terminal Cys residues, forming the bonds C1-C4 and C2-C3, were required for activity, while replacement of the other four Cys residues did not affect the activity (Fig. 3b and Extended Data Fig. 7c). Hence, whereas RLP30 only senses intact SCP^{Ss}, RE02-mediated perception requires only part of the SCP^{Ss} tertiary structure.

Consistent with the results of the individual cysteine replacements, a truncated form of SCP^{Ss}, comprising C1 to C5 (C1C5), was active in tomato and *N. benthamiana* but not in *Arabidopsis* (Fig. 3c,d and Extended Data Fig. 7d). C1C4, a variant of the protein further

truncated from both the N- and the C-terminus but still comprising the first four Cys residues, proved inactive in *Arabidopsis* but also in *N. benthamiana* and tomato (Fig. 3c,d and Extended Data Fig. 7d), indicating that in addition to the disulfide bonds also amino acids flanking the C1C4 peptide are important for immunogenic activity in solanaceous plants. Thus, SCP[Ss] is one of the very few identified ligands whose tertiary structure is important for PAMP activity similar to IF1-recognition by RLP32[14].

Intriguingly, in *B. napus, B. rapa,* and *B. oleracea* all SCP[Ss] mutants exhibited elicitor activity comparable to the wild-type SCP[Ss] (Fig. 3b and Extended Data Fig. 7c), indicating that in these Brassicaceae species SCP[Ss]-immunogenic activity is independent of cysteine-bridges and, thus, of its tertiary structure. Hence, at least two distinct SCP[Ss]-perception systems are present in Brassicaceae, one responding to intact SCP[Ss] protein (as in *Arabidopsis*), and the other one responding to a SCP[Ss]-derived peptide (as in *Brassica ssp.*). As both C1C5 and C3C8 displayed activity in Brassicaceae, we generated the 36-amino-acid peptide C3C5 spanning the overlapping region of C1C5 and C3C8 (Fig. 3a). C3C5 was found to be nearly as active as intact SCP[Ss] in *B. napus, B. rapa,* and *B. oleracea* (Fig. 3c,d and Extended Data Fig. 7d), indicating that this SCP[Ss]-fragment is sufficient to trigger immune responses in *Brassica* species. We therefore demonstrate that unlike RLP30-mediated recognition of intact SCP[Ss] in *Arabidopsis*, *Brassica* species can sense a small SCP[Ss] epitope that is distinct from the disulfide-bond containing peptide perceived in Solanaceae. In general, such large differences of sensor systems rather occur in distantly related plant families. However, similar to SCP[Ss], PG perception also differs within the Brassicaceae family and *A. thaliana*, *A. arenosa,* and *Brassica rapa* perceive immunogenic PG fragments pg9(At), pg20(Aa) and pg36(Bra), respectively[15]. Thus, the perception diversity for SCP[Ss] or PG in closely related species within the same plant family could indicate a rapid evolution of LRR-RPs in Brassicaceae.

RLP30 senses *Pseudomonas*-derived PAMPs

Intriguingly, *rlp30* mutants have been found to be more susceptible to bacterial infection with *P. syringae* pv. *phaseolicola* (*Psp* 1448A)[23]. We thus wondered whether RLP30 might also recognize a PAMP from *Pseudomonads*, despite the apparent absence of SCP[Ss] homologs in

bacteria[12]. Using the chromatographic enrichment protocol established for SCFE1[18], we could detect elicitor-activity in culture media of different *Pseudomonas* species, such as *Psp* 1448A, *Pst* DC3000, *P. fluorescens*, *P. protegens,* and *P. stutzeri* (Fig. 4a). Focusing on the activity from *Psp*, termed SCP-like^{Psp}, we observed typical immune responses such as ethylene production, MAPK activation, as well as priming for resistance towards *Pst* DC3000 infection in Arabidopsis Col-0 wild-type plants and the *rlp30-2* mutant complemented with RLP30 (Fig. 4b and Extended Data Fig. 8a). SCP-like^{Psp} also induced ethylene biosynthesis in *fls2 efr* and *rlp32-2* mutants, indicating that activity was not due to the well-established bacterial PAMPs flagellin, EF-Tu or IF1 (Extended Data Fig. 8b). In contrast, SCP-like^{Psp} had no activity in the mutant *rlp30-*2, in nine of the SCP^{Ss}-insensitive accessions, and in the *sobir1-12* and *bak1-5 bkk1-1* mutants (Fig. 4a and Extended Data Fig. 8c,d), suggesting that perception of SCP-like^{Psp} involves all the components required for perception of SCP^{Ss}. So far, our attempts to determine the molecular identity of SCP-like^{Psp} were not successful. However, much like SCP^{Ss}, the immunogenic activity of SCP-like^{Psp} was sensitive to treatment with DTT and proteases, but resistant to heat and SDS treatment, suggesting that it is likely also a protein stabilized by Cys-Cys bridges (Extended Data Fig. 8e).

RLP30 and RE02 differ in perception of SCP-like^{Psp}

SCP-like^{Psp} showed activity in *A. thaliana*, *B. rapa,* and *B. oleracea*, species of the *Brassicaceae* family that perceive SCPs and thus encode RLP30 homologs (Extended Data Fig. 8f). Interestingly, none of the species from the Solanaceae family tested showed responsiveness to bacterial SCP-like^{Psp} (Extended Data Fig. 8f). These species included *N. benthamiana, S. pennellii, S. lycopersicum, S. tuberosum and C. annuum* with functional SCP^{Ss} perception, indicating that RE02 and solanaceous homologs do not respond to SCP-like^{Psp}. Ectopic expression of RLP30 in *N. benthamiana* conferred sensitivity to SCP-like^{Psp}, but not to nlp20 which required expression of RLP23 (Fig. 4c and Extended Data Fig. 8g). Thus, RLP30, but not RE02, senses patterns from three microbial kingdoms.

RLP30 expression in *N. tabacum* confers increased resistance to bacterial, fungal and oomycete pathogens

Since RLP30 has the property of sensing PAMPs from microorganisms of three kingdoms, we introduced RLP30 into SCP^{Ss}-insensitive *N. tabacum* plants. We observed that *N. tabacum* plants transiently expressing RLP30-GFP were responsive to SCP^{Ss} and SCP-like^{Psp}, albeit with only a moderate increase in production of ethylene (Extended Data Fig. 9a,b). We wondered whether this might be due to a partial incompatibility of RLP30 with the endogenous tobacco SOBIR1. Indeed, co-expression of RLP30 with *At*SOBIR1 in *N. tabacum* established higher responses to SCP^{Ss} and SCP-like^{Psp}, whereas plants co-transformed with *RLP30* and *NbSOBIR1* or *SlSOBIR1* showed responses as plants without additional SOBIR1 (Extended Data Fig. 9a,b). Thus, we introduced *RLP30-RFP* together with the *AtSOBIR1-GFP* into *N. tabacum* and selected two stable transgenic lines (*#49* and *#55*) based on detectable expression of RLP30 and *At*SOBIR1 (Extended Data Fig. 9c). In contrast to wild-type tobacco plants, both transgenic lines clearly responded to SCPs or SCP-like^{Psp} (Fig. 5a). Importantly, when inoculated with the host-adapted, virulent bacterial pathogen *P. syringae* pv. *tabaci*, both transgenic lines exhibited less bacterial growth than wild-type plants (Fig. 5b). Moreover, compared to wild-type plants, both transgenic lines also exhibited less symptom development upon infection with the necrotrophic fungus *B. cinerea* and the oomycete *Phytophthora capsici* (Fig. 5c,d). Taken together, stable, ectopic expression of RLP30 in *N. tabacum* conferred sensitivity to SCPs and SCP-like^{Psp} and rendered these transgenic plants more resistant to destructive bacterial, fungal, and oomycete pathogens.

Concluding remarks

Plants harbor a tremendous amount of potential receptor genes, however, their characterization is strictly dependent on knowledge of respective ligands. We identified here the ligand of the previously described RLP30[18] as a secreted, small cysteine-rich protein (SCP). SCP^{Ss} is widely distributed across fungi and oomycetes[12] and its tertiary structure is important for PAMP activity, features that are rare and as combination unprecedented among known PAMPs. Additionally, SCP perception also shows unique characteristics. Extended Data Fig. 10 summarizes our

findings showing that SCP^{Ss} and its homologs do not only serve as ligands for RLP30 in Arabidopsis, but also for RE02 in *N. benthamiana* and a yet unknown *Brassica* PRR. RLP30 and RE02 share low similarity and all these PRRs moreover show distinct requirements for SCP^{Ss}: RLP30 requires intact SCP^{Ss}, Solanaceae receptors including RE02 sense the N-terminal part containing only two disulfide bonds and for SCP^{Ss} perception in Brassica (except Arabidopsis) a fragment of 36 amino acid is sufficient. Hence, the distinct perception mechanisms of the same fungal protein most likely arose through convergent evolution of LRR-RPs in different plant families. Moreover, the perception diversity for SCP^{Ss} in closely related species within the same plant family could indicate a rapid evolution of LRR-RPs in Brassicaceae.

Intriguingly, SCP^{Ss}-like sequences are not found in bacteria[12], yet RLP30, but not RE02, confers recognition of SCP-like^{Psp} from both pathogenic and beneficial *Pseudomonas* species. Hence, RLP30 is a unique receptor that can recognize most likely distinct ligands from fungi/oomycetes and bacteria.

Such a broad detection range predestines PRRs such as RLP30 as a valuable genetic tool to boost crop immunity, and RLP30 expression in *N. tabacum* does indeed confer resistance to bacterial, fungal, and oomycete infections. We propose that co-expression of heterologous PRR/co-receptor pairs may be deployed to overcome incompatibilities of ectopically expressed PRRs. Consequently, enhanced broad-spectrum resistance may be engineered as compared to expressing single PRRs alone.

Methods

Plant materials and growth conditions. *A. thaliana* plants were grown in soil for 7-8 weeks in a growth chamber under short-day conditions (8 h photoperiod, 22°C, 40%–60% humidity). *Arabidopsis* natural accessions have been previously described[24,25], mutant lines and derived complemented transgenic lines are listed in Supplementary Table 2. Solanaceae and *Brassica* plants were grown in a greenhouse at 23 °C under long-day conditions of 16 h of light and 60–70% humidity.

Peptides. Synthetic peptides flg22, nlp20, and SCP^{Ss}C3C5 (SAYTCAAPAKSHLTAESDYWVFYWGNEGVSPGVGST) (GenScript) were prepared as 10 mM stock solutions in 100% dimethyl sulfoxide (DMSO) and diluted in water to the desired concentration before use.

SCP^{Ss} identification. Partially purified SCFE1 fractions from *S. sclerotiorum* strain 1946 were purified as described[18]. The most active fractions from eight rounds of fungal culture and the two-step cation-exchange chromatography purification protocol were pooled and dialysed overnight in 2 l 25 mM MES, pH 7.0, at 4°C in a dialysis membrane (ZelluTrans, nominal MWCO: 3.5; 46mm, Roth), afterwards vacuum-filtrated through a cellulose acetate membrane (Ciro Manufacturing Corporation, pore size: 0.2µm) and loaded with a flow rate of 1ml/min onto a Source 15S 4.6/100PE column (GE Healthcare) equilibrated with buffer A (50 mM MES, pH 5.4). After washing with buffer A, bound proteins were eluted with a linear gradient of buffer B (500 mM KCl, 50 mM MES, pH 5.4; 0-50 % in 15 column volumes) and 500 µl fractions were collected using automated fractionation.

LC-MS/MS sample preparation. Three elicitor-active (B11 to B13, Extended Data Fig. 1b), and two inactive (B9 and B15) fractions of SCFE1 (in 50 mM MES buffer pH 7.0 with varying concentration of KCl, depending on the elution time point) were selected for proteomics analysis. For each fraction a sample volume of 88 µl was used, which corresponded to a total protein content per fraction from 3.9 µg (B9) to 16.0 µg (B13), as determined using the BCA protein assay kit (Thermo Fisher Scientific). All samples were reduced (10 mM DTT, 30 min, 30°C) and carbamidomethylated (55 mM CAA, 30 min, room temperature). Digestion of proteins was carried out by addition of trypsin (proteomics grade, Roche) at a 1/50 enzyme/protein ratio (w/w) and incubation at 37°C overnight. Digests were acidified by addition of 0.5 % (v/v) formic acid, and desalted using self-packed StageTips (three disks per micro-column, ø 1.5mm, C18 material, 3M Empore). The peptide eluates were dried to completeness and stored at -80°C. For LC-MS/MS analysis all samples were resuspended in 11 µl 0.1 % formic acid in HPLC grade water and 5 µl sample per measurement was injected into the mass spectrometer.

11

LC-MS/MS data acquisition. LC-MS/MS measurements were performed on a nanoLC Ultra1D+ (Eksigent, Dublin, CA) coupled online to a Q-Exactive HF-X mass spectrometer (Thermo Fisher Scientific). Peptides were loaded onto a trap column (ReproSil-pur C18-AQ, 5 μm, Dr. Maisch, 20 mm × 75 μm, self-packed) at a flow rate of 5 µl/min in 100 % solvent A (0.1 % formic acid in HPLC grade water). Subsequently, peptides were transferred to an analytical column (ReproSil Gold C18-AQ, 3 µm, Dr. Maisch, 400 mm × 75 µm, self-packed) and separated using a 50 min linear gradient from 4 % to 32 % of solvent B (0.1 % formic acid in acetonitrile and 5 % (v/v) DMSO) at 300 nl/min flow rate. Both nanoLC solvents contained 5 % (v/v) DMSO to boost the nanoESI response of peptides. The eluate from the analytical column was sprayed via a stainless-steel emitter (Thermo Fisher Scientific) at a source voltage of 2.2 kV into the mass spectrometer. The transfer capillary was heated to 275°C. The Q-Exactive HF-X was operated in data-dependent acquisition (DDA) mode, automatically switching between MS1 and MS2 spectrum acquisition. MS1 spectra were acquired over a mass-to-charge (m/z) range of 350–1400 m/z at a resolution of 60,000 using a maximum injection time of 45 ms and an AGC target value of 3e6. Up to 18 peptide precursors were isolated (isolation window 1.3 m/z, maximum injection time 25 ms, AGC value 1e5), fragmented by high-energy collision-induced dissociation (HCD) using 26 % normalized collision energy and analyzed at a resolution of 15,000 with a scan range from 200 to 2000 m/z. Precursor ions that were singly charged, unassigned, or with charge states > 6+ were excluded. The dynamic exclusion duration of fragmented precursor ions was 25 s.

LC-MS/MS data analysis. Peptide identification and quantification was performed using MaxQuant (version 1.5.3.30)[26]. MS2 spectra were searched against a *Sclerotinia sclerotiorum* protein database (assembly accession number PRJNA348385, 11130 protein sequence entries, https://www.ncbi.nlm.nih.gov/bioproject/PRJNA348385/), supplemented with common contaminants (built-in option in MaxQuant). Carbamidomethylated cysteine was set as fixed modification and oxidation of methionine and N-terminal protein acetylation as variable modifications. Trypsin/P was specified as proteolytic enzyme. Precursor tolerance was set to 4.5 ppm, and fragment ion tolerance to 20 ppm. Results were adjusted to 1 % false discovery rate (FDR) on peptide spectrum match (PSM) and protein level employing a target-decoy

approach using reversed protein sequences. The minimal peptide length was defined as 7 amino acids, the "match-between-run" function was enabled (default settings). To assess and quantitatively compare the concentrations of the detected proteins the "intensity based absolute quantification" (iBAQ)[27] algorithm was employed. The detected 22 proteins were further filtered and prioritized according to the following characteristics: 1) good correlation between the elicitor activity profile and the measured mass spectrometric protein intensity over the five investigated SCFE1 fractions; 2) presence of a predicted signal peptide sequence (using the SignalP v.6.0 server)[28]; 3) protein molecular weight in the range between 10 to 30 kDa; 4) high cysteine content relative to protein length; 5) detection of at least two unique peptides per protein (Supplementary Table 1).

SCP^{Ss} expression and purification. For expression of SCP^{Ss} in *N. benthamiana* leaves, the SCP^{Ss} sequence was cloned into the pBIN-plus vector with a C-terminal GFP tag[15]. *Agrobacterium tumefaciens* strain GV3101 carrying pBIN-plus-SCP^{Ss} was infiltrated into leaves of 4-6-week-old *N. benthamiana* plants. At 48 hours post agro-infiltration leaves were vacuum-infiltrated with 0.5 M NaCl, 0.4 M Na_2HPO_4 and 0.4 M NaH_2PO_4 and the apoplastic wash-fluid containing SCP^{Ss} (SCP^{Ss}-AWF) was collected by centrifugation at 1500g for 20 min and 4°C. For recombinant protein expression in *Pichia pastoris* KM71H (Multi-Copy Pichia Expression Kit Instructions, Thermo Fisher Scientific), constructs encoding *SCP^{Ss}*, *SCP^{Bc}*, *SCP^{Pi}*, truncated *SCP^{Ss}* versions and cysteine-to-serine replacements (all without signal peptide and Stop codon) were cloned into the secretory expression plasmid pPICZalphaA (Thermo Fisher Scientific). Individual cysteine to serine replacements in SCP^{Ss} were amplified from synthetic genes (gBlocks, Integrated DNA Technologies) using primers extended by restriction sites *Eco*RI and *Bam*HI and cloned into pPICZalphaA. Sequence information on primers and synthetic genes used in this study can be found in Supplementary Tables 3 and 5. Protein purification from *P. pastoris* culture medium was achieved by affinity chromatography on 5 ml HisTrapFF column (GE Healthcare; equilibrated in 20 mM Tris-HCl, 200 mM NaCl, pH 8.0), following washing (20 mM Tris-HCl, 200 mM NaCl, 20 mM imidazole, pH 8.0) and elution (buffer gradient 0-500 mM imidazole in equilibration buffer). Recombinant protein expression was verified by concentration

13

determination using the Bradford method and by Western Blot analysis using the anti-His antibody (dilution 1:1000, Abcam).

SCP-like purification from *Pseudomonas* ssp. *Pseudomonas* strains (*Pseudomonas syringae* pv. *tomato* DC3000, *Pseudomonas syringae* pv. *phaseolicola* 1448A, *Pseudomonas protegens* Pf-5, *Pseudomonas fluorescens* SBW25, *Pseudomonas stutzeri* DSM10701) were grown in baffled flasks (200 ml medium in 1 l flask) in liquid PDB medium (24 g/l Potato Dextrose Broth, Duchefa) for 12 h at 21°C with 210 rpm shaking. The culture medium was centrifuged at 6000 rpm for 20 min and then vacuum-filtrated through a filter paper (MN 615, Macherey-Nagel) and subjected to a two-step cation exchange chromatography protocol using an ÄKTA Explorer FPLC system (GE Healthcare) kept at 4°C. In a first step, the culture filtrate was loaded onto HiTrap SP FF column(s) (GE Healthcare) equilibrated in buffer A (50 mM MES, pH 5.4) at a flow rate of up to 15 ml/min. After washing with buffer A, a 100 % elution step with buffer B (500 mM KCl, 50 mM MES, pH 5.4) was performed at a flow rate of 1-2 ml/min and the elution peak was monitored with OD280nm, OD254nm and OD214nm and collected manually. The collected eluate was dialysed against 2 l 25 mM MES, pH 5.4, overnight at 4°C in a dialysis membrane (ZelluTrans, nominal MWCO: 3.5; 46 mm, Roth), afterwards vacuum-filtrated through a cellulose acetate membrane (Ciro Manufacturing Corporation, pore size: 0.2 µm) and loaded with a flow rate of 1 ml/min onto a Source 15S 4.6/100PE column (GE Healthcare) equilibrated with buffer A. After washing with buffer A the bound proteins were eluted with a linear gradient of buffer B (0 to 50 % in 10 column volumes) and 500 µl fractions were collected using automated fractionation.

Generation of transgenic plants. For the generation of transgenic *rlp30-2* lines expressing *p35S::RE02-GFP*, the coding sequence of *RE02* extended by *Bsa*I cleavage sites (Supplementary Table 3) was cloned into the pGEM®-T vector (Promega). The cauliflower mosaic virus 35 promoter, *RE02* coding sequence and GFP-tag were assembled via golden gate cloning in the vector LII_F_1-2_-_BB10c[29] and constructs were transformed into *rlp30-2* by floral dipping.

For 35S-promoter-driven stable expression of *RLP30-YFP* in *rlp30-2* mutants or *RLP30-RFP* and *SOBIR1-GFP* in *N. tabacum L.* var. Samsun NN, *RLP30* and *SOBIR1* coding sequences were first cloned into pCR™8/GW/TOPO™ (Thermo Fisher Scientific) and subsequently fused via Gateway cloning to a C-terminal YFP (pB7YWG2[30]), RFP (pB7RWG2[30]) or GFP (pK7FWG2[30]), respectively. Primers used are listed in Supplementary Table 3. Stable transformation was performed as described previously[19]. Protein expression in transgenic lines was verified by immunoblotting using anti-RFP (Abcam) and anti-GFP (Thermo Fisher Scientific) antibodies and response to SCFE1.

Transient protein expression and co-immunoprecipitations. For 35S-promoter-driven transient protein expression in *N. benthamiana or N. tabacum*, coding sequences of respective genes were amplified using the primers listed in Supplementary Table 3, cloned into pCR™8/GW/TOPO™ (Thermo Fisher Scientific) and subsequently recombined via Gateway cloning into pGWB5 (C-terminal GFP-tag), pGWB14 (C-terminal HA-tag), or pGWB17 (C-terminal Myc-tag)[31]. Likewise, a pENTR/D-Topo (Thermo Fisher Scientific) clone containing the coding sequence for *NbSOBIR1*[32] was recombined with pGWB14, *p35S::SlSOBIR1-HA* in pGWB14 has been described previously[33]. Transient protein expression in *Nicotiana* and constructs for *AtSOBIR1-HA*, *BAK1-myc* and *RLP23-GFP* have been previously described[19]. For SCP^{Ss}-binding assays, SCP^{Ss}-Myc (pGWB17) together with RLP30-GFP (pGWB5) from different *Arabidopsis* accessions was transiently co-expressed in *N. benthamiana*. On day 2, leaf material was harvested and protein extracts were subjected to immunoprecipitation using GFP-Trap beads (ChromoTek). 200 mg ground leaf material was subjected to protein extraction and immunoprecipitation using GFP-Trap beads (ChromoTek)[19]. Proteins were detected by immunoblotting with tag-specific antibodies raised against epitope tags GFP (dilution 1:5000), HA (dilution 1:3000) or Myc (dilution 1:5000, all Thermo Fisher Scientific), followed by staining with secondary antibodies coupled to horseradish peroxidase and ECL (Cytiva).

Plant immune responses. Determination of the accumulation of ethylene and reactive oxygen species and MAPK activity assays were performed as previously described[34]. Ethylene

15

production was induced in three leaf pieces floating on 0.5 ml 20 mM MES buffer pH 5.7 and the indicated elicitors. After incubation for 4 h, 1 ml air was drawn from sealed assay tubes and the ethylene content was measured by gas chromatography (GC-14A, Shimadzu). ROS accumulation was measured in one leaf piece per well placed in a 96-well plate (Greiner BioOne) containing 100 μl of a solution with 20 μM luminol derivative L-012 (Wako Pure Chemical Industries) and 20 ng ml^{-1} horseradish peroxidase (Applichem). Luminescence was measured in 2 min intervals both before (background) and for up to 60 min after PAMP or mock treatment using a Mithras LB 940 luminometer (Berthold Technologies). For MAPK activity assays, treated leaf material was harvested after indicated times and frozen in liquid nitrogen. Proteins were extracted with 20 mM Tris-HCl pH 7.5, 150 mM NaCl, 1 mM EDTA, 1 % Triton X-100, 0.1 % SDS, 5 mM DTT, Complete Protease Inhibitor Mini, EDTA-free (Roche), PhosStop Phosphatase Inhibitor Cocktail (Roche), separated via 10 % SDS-PAGE, and transferred to nitrocellulose. Activated MAPKs were detected by protein blotting using the rabbit anti-phospho-p44/42-MAPK antibody (Cell Signalling Technology, 1:1000 dilution).

Plant infections. Leaves of 6- to 8-week-old Arabidopsis plants were primed by leaf infiltration with 1 μM nlp20, 1 μM SCP^{Ss} or SCP-like^{Psp}, or water (mock treatment) and after 24 h inoculated with *Pseudomonas syringae* pv. *tomato* DC3000 (*Pst* DC3000) by leaf infiltration with a final cell density of 10^4 colony-forming units (CFU) per ml 10 mM MgCl$_2$. Bacterial populations were determined 3 d after infiltration[35]. *N. tabacum* plants were likewise infected with *P. syringae* pv. *tabaci*[36] at a final cell density of 10^5 CFU/ml and harvested after 4 days. For fungal infection, spores of *B. cinerea* isolate B05.10 or SCP^{Bc} depletion mutant *ΔSCP^{Bc}/Bcplp1*[21] (lines 45 and 46) were diluted to a final concentration of 5 x 10^6 spores per ml in potato dextrose broth and 5-μl drops were used for leaf inoculation. Lesion sizes were determined after 2 d by determining the average lesion diameter. *N. tabacum* leaves inoculated with 0.8 cm fresh mycelial plugs of *Phytophthora capsici* grown on V8 juice agar were clipped and kept in the dark in plastic boxes to obtain high humidity. Lesion diameters were measured at 48 hpi using UV light.

For virus-induced gene silencing (VIGS), a 300 bp fragment of *RE02* was amplified using primers listed in Supplementary Table 3 and cloned into vector pYL156[37] (*TRV2::RE02*), the

TRV2::GUS control construct has been previously described[32]. Agrobacterium-mediated VIGS was performed as described[32]. Gene silencing was verified by measuring *RE02* transcript levels versus *NbActin* transcript levels using quantitative RT-PCR with primers listed in Supplementary Table 4.

Data availability

All data are available in the main text, extended data or the Supplementary Information. Source data are provided with this paper. The LC-MS/MS data files as well as the MaxQuant output files have been deposited to the ProteomeXchange Consortium via the PRIDE partner repository (https://www.ebi.ac.uk/pride/) and can be accessed using the identifier PXD036013.

Acknowledgements

Author contributions

Y.Y., C.E.S., G.F. and A.A.G. conceived and designed the experiments; Y.Y., C.E.S., B.L., D.K., T.L. and W.Z. conducted experiments; Y.Y., C.E.S., G.F., C.L., M.F.S., M.H., R.H. and A.A.G. analyzed data; B.G. and H.G. provided materials; G.F. and T.N. revised the manuscript and Y.Y., C.E.S., and A.A.G. wrote the manuscript. All authors discussed the results and commented on the manuscript.
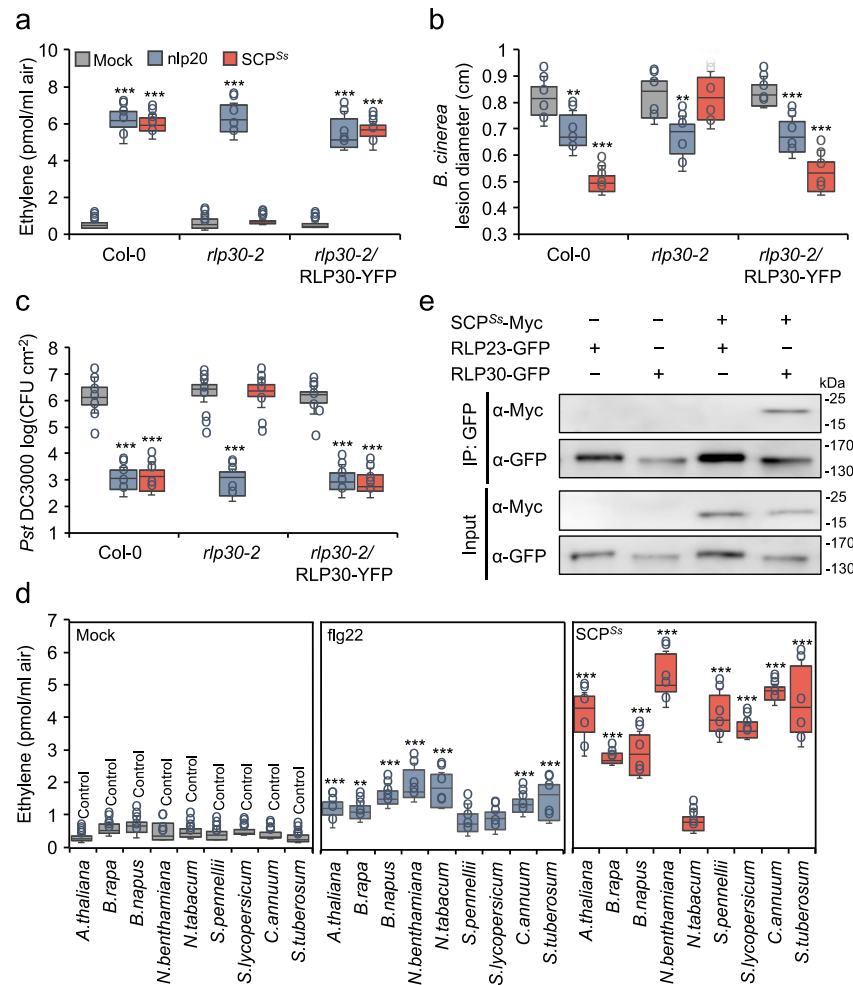
References

1   Dodds, P. N. & Rathjen, J. P. Plant immunity: towards an integrated view of plant-pathogen interactions. *Nat Rev Genet* **11**, 539-548, doi:10.1038/nrg2812 (2010).

2   Jones, J. D. & Dangl, J. L. The plant immune system. *Nature* **444**, 323-329, doi:10.1038/nature05286 (2006).

3   Ngou, B. P. M., Ding, P. & Jones, J. D. G. Thirty years of resistance: Zig-zag through the plant immune system. *Plant Cell* **34**, 1447-1478, doi:10.1093/plcell/koac041 (2022).

4   Albert, I., Hua, C., Nürnberger, T., Pruitt, R. N. & Zhang, L. Surface Sensor Systems in Plant Immunity. *Plant physiology* **182**, 1582-1596, doi:10.1104/pp.19.01299 (2020).

5   Saijo, Y., Loo, E. P. & Yasuda, S. Pattern recognition receptors and signaling in plant-microbe interactions. *Plant J* **93**, 592-613, doi:10.1111/tpj.13808 (2018).

6   Wan, W. L., Fröhlich, K., Pruitt, R. N., Nürnberger, T. & Zhang, L. Plant cell surface immune receptor complex signaling. *Current opinion in plant biology* **50**, 18-28, doi:10.1016/j.pbi.2019.02.001 (2019).

7   Gust, A. A. & Felix, G. Receptor like proteins associate with SOBIR1-type of adaptors to form bimolecular receptor kinases. *Current opinion in plant biology* **21**, 104-111, doi:10.1016/j.pbi.2014.07.007 (2014).

8   Chinchilla, D., Shan, L., He, P., de Vries, S. & Kemmerling, B. One for all: the receptor-associated kinase BAK1. *Trends in plant science* **14**, 535-541, doi:10.1016/j.tplants.2009.08.002 (2009).

9   Zhou, J. M. & Zhang, Y. Plant Immunity: Danger Perception and Signaling. *Cell* **181**, 978-989, doi:10.1016/j.cell.2020.04.028 (2020).

10   Böhm, H. *et al.* A conserved peptide pattern from a widespread microbial virulence factor triggers pattern-induced immunity in Arabidopsis. *PLoS pathogens* **10**, e1004491, doi:10.1371/journal.ppat.1004491 (2014).

11   Ma, Z. *et al.* A Phytophthora sojae Glycoside Hydrolase 12 Protein Is a Major Virulence Factor during Soybean Infection and Is Recognized as a PAMP. *Plant Cell* **27**, 2057-2072, doi:10.1105/tpc.15.00390 (2015).

12   Nie, J., Yin, Z., Li, Z., Wu, Y. & Huang, L. A small cysteine-rich protein from two kingdoms of microbes is recognized as a novel pathogen-associated molecular pattern. *New Phytol* **222**, 995-1011, doi:10.1111/nph.15631 (2019).

13   Seidl, M. F. & Van den Ackerveken, G. Activity and Phylogenetics of the Broadly Occurring Family of Microbial Nep1-Like Proteins. *Annu Rev Phytopathol* **57**, 367-386, doi:10.1146/annurev-phyto-082718-100054 (2019).

14   Fan, L. *et al.* Genotyping-by-sequencing-based identification of Arabidopsis pattern recognition receptor RLP32 recognizing proteobacterial translation initiation factor IF1. *Nat Commun* **13**, 1294, doi:10.1038/s41467-022-28887-4 (2022).

15   Zhang, L. *et al.* Distinct immune sensor systems for fungal endopolygalacturonases in closely related Brassicaceae. *Nature plants* **7**, 1254-1263, doi:10.1038/s41477-021-00982-2 (2021).

16   Albert, M. *et al.* Regulation of cell behaviour by plant receptor kinases: Pattern recognition receptors as prototypical models. *European journal of cell biology* **89**, 200-207, doi:10.1016/j.ejcb.2009.11.015 (2010).

17   Sanchez-Vallet, A., Mesters, J. R. & Thomma, B. P. The battle for chitin recognition in plant-microbe interactions. *FEMS Microbiol Rev* **39**, 171-183, doi:10.1093/femsre/fuu003 (2015).

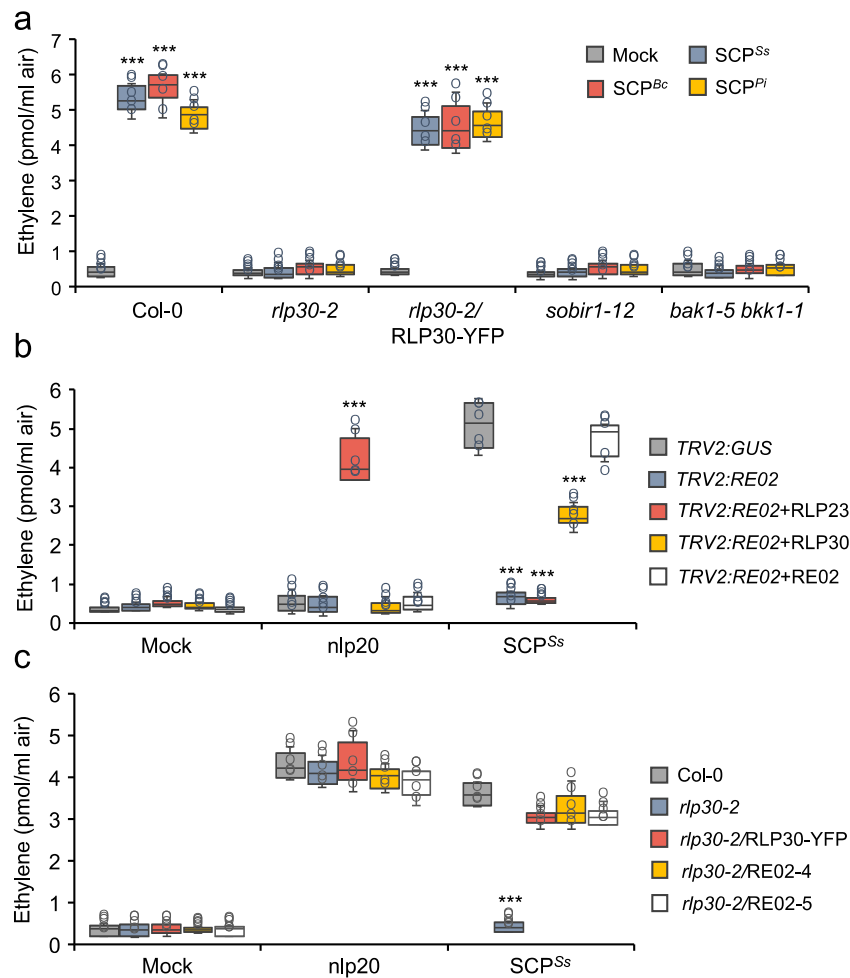18   Zhang, W. *et al.* Arabidopsis receptor-like protein30 and receptor-like kinase suppressor of BIR1-

1/EVERSHED mediate innate immunity to necrotrophic fungi. *Plant Cell* **25**, 4227-4241, doi:10.1105/tpc.113.117010 (2013).

19   Albert, I. *et al.* An RLP23-SOBIR1-BAK1 complex mediates NLP-triggered immunity. *Nature plants* **1**, 15140, doi:10.1038/nplants.2015.140 (2015).

20   Stergiopoulos, I. & de Wit, P. J. Fungal effector proteins. *Annu Rev Phytopathol* **47**, 233-263, doi:10.1146/annurev.phyto.112408.132637 (2009).

21   Leisen, T. *et al.* Multiple knockout mutants reveal a high redundancy of phytotoxic compounds contributing to necrotrophic pathogenesis of Botrytis cinerea. *PLoS pathogens* **18**, e1010367, doi:10.1371/journal.ppat.1010367 (2022).

22   Nie, J. *et al.* A receptor-like protein from Nicotiana benthamiana mediates VmE02 PAMP-triggered immunity. *New Phytol* **229**, 2260-2272, doi:10.1111/nph.16995 (2021).

23   Wang, G. *et al.* A genome-wide functional investigation into the roles of receptor-like proteins in Arabidopsis. *Plant physiology* **147**, 503-517, doi:10.1104/pp.108.119487 (2008).

24   Cao, J. *et al.* Whole-genome sequencing of multiple Arabidopsis thaliana populations. *Nat Genet* **43**, 956-963, doi:10.1038/ng.911 (2011).

25   Nordborg, M. *et al.* The pattern of polymorphism in Arabidopsis thaliana. *Plos Biology* **3**, 1289-1299, doi:10.1371/journal.pbio.0030196 (2005).

26   Cox, J. & Mann, M. MaxQuant enables high peptide identification rates, individualized p.p.b.-range mass accuracies and proteome-wide protein quantification. *Nat Biotechnol* **26**, 1367-1372, doi:10.1038/nbt.1511 (2008).

27   Schwanhausser, B. *et al.* Global quantification of mammalian gene expression control. *Nature* **473**, 337-342, doi:10.1038/nature10098 (2011).

28   Teufel, F. *et al.* SignalP 6.0 predicts all five types of signal peptides using protein language models. *Nat Biotechnol* **40**, 1023-1025, doi:10.1038/s41587-021-01156-3 (2022).

29   Binder, A. *et al.* A modular plasmid assembly kit for multigene expression, gene silencing and silencing rescue in plants. *PLoS One* **9**, e88218, doi:10.1371/journal.pone.0088218 (2014).

30   Karimi, M., De Meyer, B. & Hilson, P. Modular cloning in plant cells. *Trends in plant science* **10**, 103-105, doi:10.1016/j.tplants.2005.01.008 (2005).

31   Nakagawa, T. *et al.* Development of series of gateway binary vectors, pGWBs, for realizing efficient construction of fusion genes for plant transformation. *Journal of bioscience and bioengineering* **104**, 34-41, doi:10.1263/jbb.104.34 (2007).

32   Liebrand, T. W. *et al.* Receptor-like kinase SOBIR1/EVR interacts with receptor-like proteins in plant immunity against fungal infection. *Proc Natl Acad Sci U S A* **110**, 10010-10015, doi:10.1073/pnas.1220015110 (2013).

33   Postma, J. *et al.* Avr4 promotes Cf-4 receptor-like protein association with the BAK1/SERK3 receptor-like kinase to initiate receptor endocytosis and plant immunity. *New Phytol* **210**, 627-642, doi:10.1111/nph.13802 (2016).

34   Wan, W. L. *et al.* Comparing Arabidopsis receptor kinase and receptor protein-mediated immune signaling reveals BIK1-dependent differences. *New Phytol* **221**, 2080-2095, doi:10.1111/nph.15497 (2019).

35   Schlöffel, M. A. *et al.* The BIR2/BIR3-Associated Phospholipase Dgamma1 Negatively Regulates Plant Immunity. *Plant physiology* **183**, 371-384, doi:10.1104/pp.19.01292 (2020).

36   Oh, H. S. & Collmer, A. Basal resistance against bacteria in Nicotiana benthamiana leaves is accompanied by reduced vascular staining and suppressed by multiple Pseudomonas syringae

type III secretion system effector proteins. *Plant J* **44**, 348-359, doi:10.1111/j.1365-313X.2005.02529.x (2005).

37   Liu, Y., Schiff, M., Marathe, R. & Dinesh-Kumar, S. P. Tobacco Rar1, EDS1 and NPR1/NIM1 like genes are required for N-mediated resistance to tobacco mosaic virus. *Plant J* **30**, 415-429, doi:10.1046/j.1365-313x.2002.01297.x (2002).
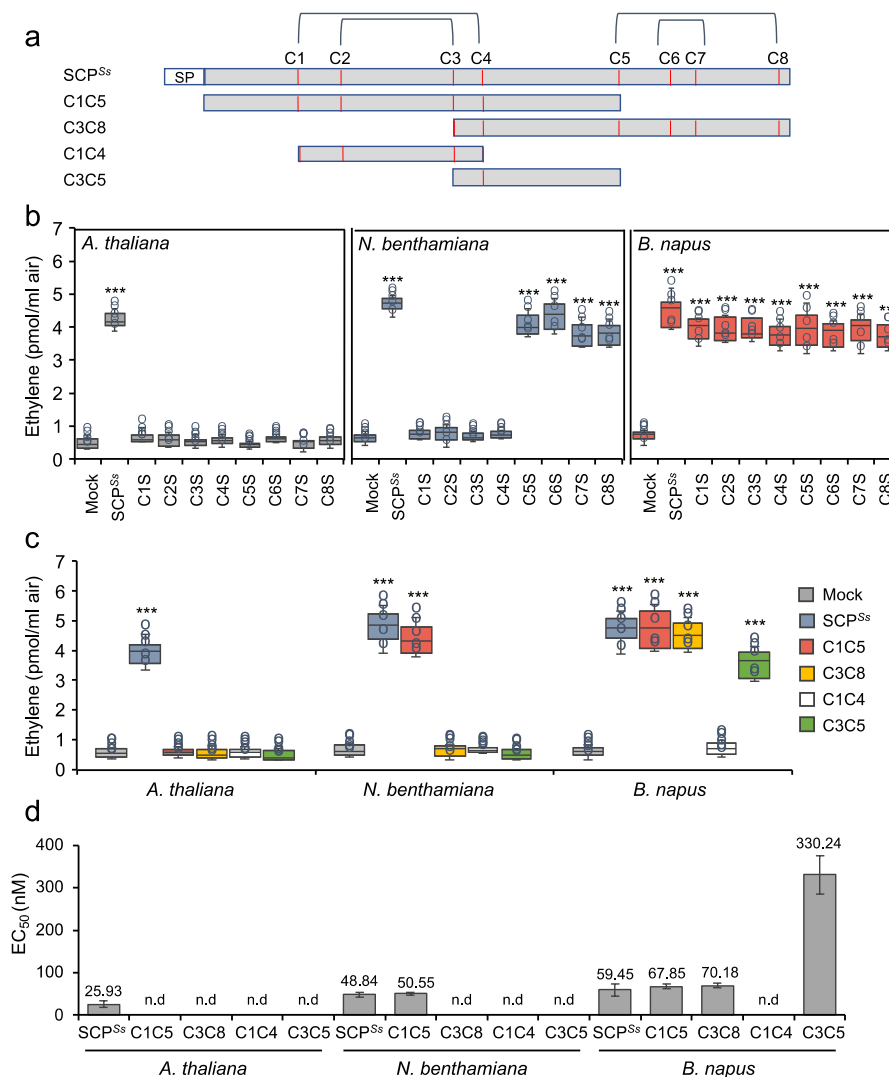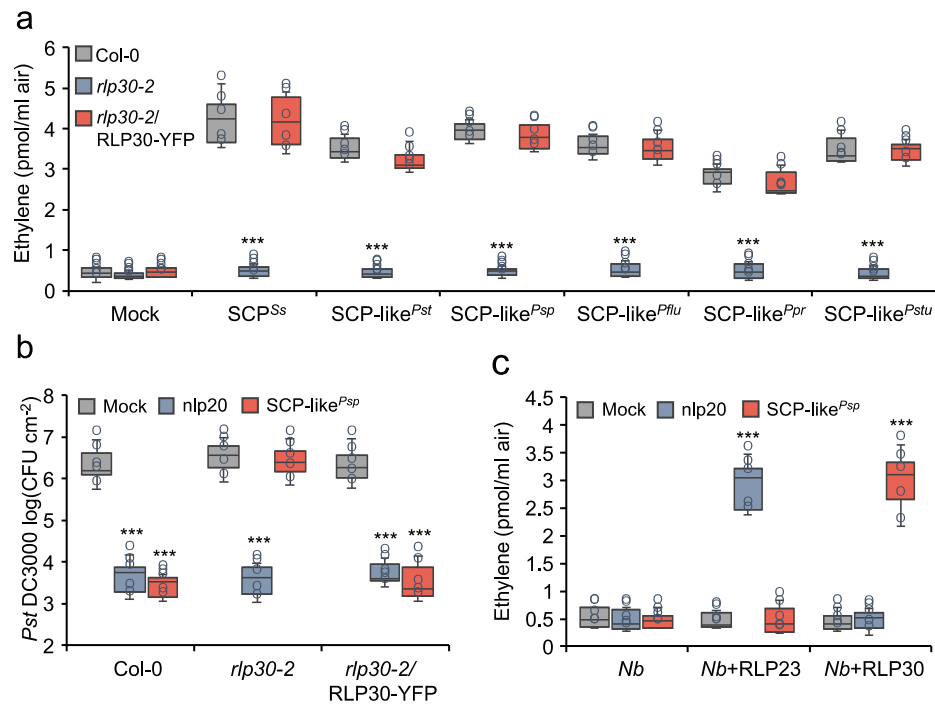
Main Figures

Fig. 1 SCP^{Ss} is immunogenic and binds to RLP30. a, Ethylene accumulation in Arabidopsis Col-0 wild-type plants, *rlp30-2* mutants, or an *rlp30-2* line complemented with a *p35S::RL30-YFP* construct 4 h after treatment with water (mock), 1 µM nlp20, or 1 µM *P. pastoris*-expressed SCP^{Ss}. **b,** *B. cinerea* infected area as determined by lesion diameter on day 2 after 24 h-treatment of Col-0 wild-type plants, *rlp30-2* mutants or the *rlp30-2/RLP30-YFP* complementation line with water (mock), 1 µM nlp20, or 1 µM SCP^{Ss}. **c,** Bacterial growth in plants pre-treated with water (mock), 1 µM nlp20, or 1 µM SCP^{Ss} 24 h before infiltration of *Pst* DC3000. Bacteria (colony forming units, CFU) were quantified in extracts of leaves 3 days after inoculation. **d,** Ethylene accumulation in plants of the Brassicaceae and Solanaceae family 4 h after treatment with water (mock), 1 µM flg22, or 1 µM SCP^{Ss}. **e,** Ligand-binding assay in *N. benthamiana* transiently co-expressing SCP^{Ss}-myc and either RLP30-GFP or RLP23-GFP. Leaf protein extracts (Input) were used for co-immunoprecipitation with GFP-trap beads (IP:GFP) and immunoblotting with tag-specific antibodies. For a-d, data points are indicated as dots (n = 6 for a, b, d; n = 20 for c) and plotted as box plots (centre line, median; bounds of box, the first and third quartiles; whiskers, 1.5 times the interquartile range; error bar, minima and maxima). Statistically significant differences from mock treatments in the respective plants are indicated (two-sided Student's t-test, **$P \leq 0.01$, ***$P \leq 0.001$). All assays were performed at least three times with similar results.

Fig. 2 SCPs are sensed by RE02 and RLP30. A, Ethylene accumulation in *Arabidopsis* wild-type plants (Col-0) or indicated mutants 4 h after treatment with water (mock), 1 μM nlp20, 1 μM SCP^{Ss}, or homologs from *B. cinerea* (*Bc*) and *Phytophthora infestans* (*Pi*). **b,** *N. benthamiana* plants were silenced for *RE02*, and transiently transformed with *RLP23-GFP*, *RLP30-GFP*, or *RE02-GFP*, respectively. The *TRV2:GUS* construct was used as a control. Ethylene production was measured 4 h after treatment with water (mock), 1 μM nlp20, or 1 μM SCP^{Ss}. **c,** Ethylene accumulation in *Arabidopsis rlp30-2* mutants or lines stably expressing RLP30-YFP or RE02-GFP (line 4 and 5) 4 h after treatment with water (mock), 1 μM nlp20, or 1 μM SCP^{Ss}. Data points are indicated as dots (*n* = 6) and plotted as box plots (centre line, median; bounds of box, the first and third quartiles; whiskers, 1.5 times the interquartile range; error bar, minima and maxima). Statistically significant differences from control treatments are indicated (two-sided Student's t-test, ***$P \leq 0.001$). Each experiment was repeated three times with similar results.
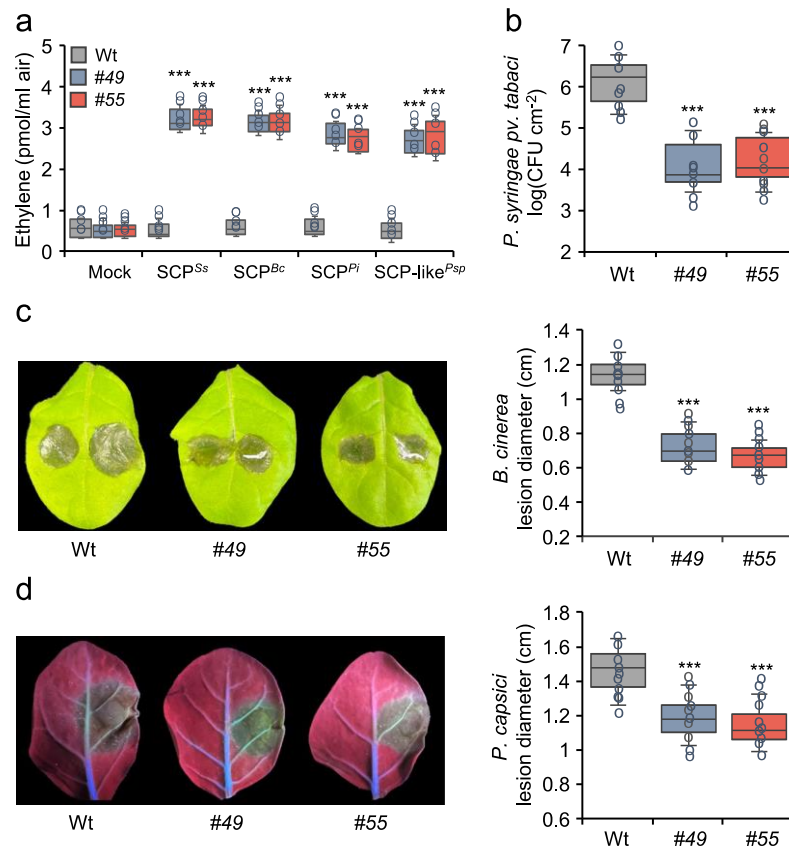
Fig. 3 SCP^{Ss} sensing differs in Brassicaceae and Solanaceae. a, Schematic representation of SCP^{Ss} and derived truncations C1C5, C3C8, C1C4 and C3C5. Cysteine (C) residues are numbered and indicated as red lines, predicted disulphide bridges (DB, http://clavius.bc.edu/~clotelab/DiANNA/) are shown on top. SP, signal peptide. **b,c,** Ethylene accumulation in *A. thaliana* Col-0, *N. benthamiana* or *B. napus* wild-type plants after 4 h treatment with water (mock), 1 µM SCP^{Ss}, and SCP^{Ss} with individual cysteine to serine mutations (**b**) or SCP^{Ss} truncations depicted in **a** (**c**). Data points are indicated as dots (n = 6 for b; n = 6 for c) and plotted as box plots (centre line, median; bounds of box, the first and third quartiles; whiskers, 1.5 times the interquartile range; error bar, minima and maxima). Statistically significant differences from mock treatments in the respective plants are indicated (two-sided Student's t-test, ***P ≤ 0.001). **d,** Determination of EC$_{50}$ values of SCP^{Ss} and the various SCP^{Ss} truncations using ethylene accumulation in *A. thaliana*, *N. benthamiana*, or *B. napus* plants after treatment with increasing concentrations of recombinant SCP^{Ss} versions (produced in *Pichia*) or synthetic C3C5 (n.d, activity not detectable). Each experiment was repeated three times with similar results.

Fig. 4 *Pseudomonads* produce a RLP30-dependent elicitor activity. A, Ethylene accumulation in Col-0 wild-type plants, *rlp30-2* mutants or an *rlp30-2* line complemented with a *p35S::RL30-YFP* construct 4 h after treatment with water (mock), 1 μM SCP^{Ss} or 1.5 μg/ml SCP-like from *Pseudomonas syringae* pv. *tomato (Pst)*, *P. syringae* pv. *phaseolicola (Psp)*, *P. fluorescens (Pflu)*, *P. protegens (Ppr)*, and *P. stutzeri (Pstu)*. **b,** Bacterial growth in Col-0 wild-type plants, *rlp30-2* mutants, or the *rlp30-2/RLP30-YFP* complementation line treated with water (mock), 1 μM nlp20, or 1.5 μg/ml SCP-like^{Psp} 24 h before infiltration of *Pst* DC3000. Bacteria (colony forming units, CFU) were quantified in extracts of leaves 3 days after inoculation. **c,** Ethylene accumulation in *N. benthamiana* (*Nb*) plants transiently expressing RLP23-GFP or RLP30-GFP and treated for 4 h with water (mock), 1 μM nlp20, or 1.5 μg/ml SCP-like^{Psp}. Data points are indicated as dots (*n* = 6 for a, c; *n* = 20 for b) and plotted as box plots (centre line, median; bounds of box, the first and third quartiles; whiskers, 1.5 times the interquartile range; error bar, minima and maxima). Statistically significant differences from Col-0 plants (**a**) or mock treatments (**b,c**) are indicated (two-sided Student's t-test, ***$P \leq 0.001$). Each experiment was repeated three times with similar results.

Fig. 5 RLP30 expression in *N. tabacum* confers increased resistance to bacterial, fungal, and oomycete pathogens. a, Ethylene accumulation in *N. tabacum* wild-type plants (Wt) or two transgenic lines (*#49* and *#55*) stably expressing RLP30-RFP and SOBIR1-GFP after 4 h treatment with water (mock), 1 μM SCP from indicated sources, or 1.5 μg/ml SCP-like^{Psp}. **b,** Bacterial growth of *P. syringae* pv. *tabaci* in *N. tabacum* wild-type plants (Wt) or transgenic *RLP30/SOBIR1* lines (#49 and #55). Bacteria (colony forming units, CFU) were quantified in extracts of leaves 3 days after inoculation. **c,** *B. cinerea* infected area on leaves of *N. tabacum* wild-type plants (Wt) or transgenic *RLP30/SOBIR1* lines (left, shown are representative leaves) and determination of lesion diameter on day 2 after drop inoculation (right). **d,** Growth of *Phytophthora capsici* on leaves of *N. tabacum* wild-type plants (Wt) or transgenic *RLP30/SOBIR1* lines by determination of lesion size (right) of lesions observed under UV light (left, shown are representative leaves) on day 2 after drop inoculation. Data points are indicated as dots (*n* = 6 for a; *n* = 20 for b, *n* = 10 for c, d) and plotted as box plots (centre line, median; bounds of box, the first and third quartiles; whiskers, 1.5 times the interquartile range; error bar, minima and maxima). Statistically significant differences from wild-type (Wt) plants are indicated (two-sided Student's t-test, ****P* ≤ 0.001). Each experiment was repeated three times with similar results.